THE ACCELERATED CORROSION OF CANDU OUTLET FEEDERS - OBSERVATIONS, POSSIBLE MECHANISMS AND POTENTIAL REMEDIES

By

D.H. Lister
University of New Brunswick
Fredericton, N.B.

J. Slade
Point Lepreau Generating Station
St. John, New Brunswick

and

N. Arbeau
University of New Brunswick
Fredericton, N.B.

ABSTRACT

The outlet feeders at all of the CANDU-6 reactors and at several of the Ontario Hydro reactors are corroding at rates that are much higher than were ever predicted from measurements in autoclaves or out-reactor loops. Over the last year since the phenomenon was discovered a flurry of activity at the operating reactors and research laboratories has indicated the origins of the important mechanisms involved; at the same time, clues as to possible remedies have emerged. A summary of some of that activity, centred on the experience at the CANDU-6 at Point Lepreau and the research at the University of New Brunswick, is presented here.

THE ACCELERATED CORROSION OF CANDU OUTLET FEEDERS - OBSERVATIONS, POSSIBLE MECHANISMS AND POTENTIAL REMEDIES

By

D.H. Lister
University of New Brunswick
Fredericton, N.B.

J. Slade
Point Lepreau Generating Station
St. John, New Brunswick

and

N. Arbeau
University of New Brunswick
Fredericton, N.B.

INTRODUCTION

The routine survey measurements of feeder wall thickness, which have been carried out with ultrasonic techniques according to CSA Standard N285.4 "Periodic Inspection of Nuclear Power Plant Components" on inlet and outlet feeders at CANDU reactors since their start-up, have shown no untoward corrosion. These measurements are usually made close to the reactor inlet and outlet headers at places that are reasonably accessible; however, after measurements were made at Point Lepreau during the extended outage of 1995-96 at places close to the reactor face, it became clear that excessive thinning of the first few metres of the outlet feeders was widespread. Measurements at the other CANDU-6s, at Darlington and at Bruce have confirmed that those reactors also are experiencing thinning at rates far in excess of what was predicted from early measurements in autoclaves or out-reactor loops. In fact, thinning rates greater than 150 μm/a have been estimated for some feeders by comparing present wall thicknesses with best estimates of starting thicknesses derived from the known characteristics of the carbon steel piping that was originally specified and installed (no routine measurements were ever made close to the reactor, so base lines for wall thickness at that location were never established). By contrast, it should be noted that the accepted values for carbon steel corrosion rate obtained from laboratory testing under-conditions similar to those of CANDU coolant were generally below 10 μm/a(1-3).

Since the discovery of these excessive thinning rates reactor operators and designers have intensified their activities related to the monitoring of feeder piping and are correlating thinning rates with operating variables; also, researchers have begun investigations into the underlying mechanisms with a view to understanding the process so that remedies can be formulated.

The Point Lepreau CANDU in New Brunswick has been at the forefront of the reactor studies and has now accumulated a considerable amount of information. At the same time, at the University of New Brunswick, researchers have carried out preliminary scoping studies and proposed a tentative model of the phenomenon that extends somewhat the conventional explanation based on a flow-assisted-corrosion (FAC) mechanism like the ones invoked routinely for secondary-coolant systems. This paper outlines the New Brunswick findings.

OBSERVATIONS AT POINT LEPREAU GENERATING STATION (PLGS)

The wall thickness of the Point Lepreau feeders has been measured by staff of the New Brunswick Research and Productivity Council (RPC), who use an ultrasonic technique with a reputed accuracy of ±10 μm. In the field, accuracies in the order of ±100 μm are probably obtained. The precision of the measurements is improved by means of a flexible plastic template which is split in order to fit around the piping and is moulded to the shape of the bends that occur just downstream of the Grayloc fitting where the piping is connected to the fuel channel end fitting. The template is perforated with holes that are the same size as the ultrasonic detector head (see Figure 1).

Most of the measurements have been made at the first and second bends, for it is there that the maximum thinning rate has been anticipated (because of the high turbulence of the coolant leaving the fuel channel) and it is there that the wall thickness was initially the lowest (because of the pipe bending which thins the metal at the outside of the bend, i.e., at the extrados). The piping for these lower outlet feeders is either of 2" nominal outside diameter (in 60 channels) or 2.5" (in 320 channels). As Figure 2 demonstrates, the feeder arrangement in this area is congested, making it difficult on many channels to apply the ultrasonic detector in a full circumferential scan to any distance away from the Grayloc. Furthermore, radiation fields at the reactor face and towards the headers tend to be quite high, hampering the monitoring even more.

In spite of the difficulties, many measurements were made at PLGS in 1996. On 64 outlet and three inlet feeders, about 7,000 determinations of wall thickness were made in all. In addition, early in 1997 a heavy-water leak was traced to outlet feeder S08, which had developed a crack at the first bend after the Grayloc; the replacement of about a metre of the pipe has provided a length of thinned feeder for detailed examination. And finally, one outlet feeder - F11 - was monitored up to 3 m or so downstream of the Grayloc. This provided information on the thinning rate beyond the first bends, including some straight sections.

The major findings to date of the PLGS measurement program are as follows:

1. Outlet feeders are corroding much more rapidly than inlets. All of the three inlet feeders that were measured indicated corrosion rates averaged over the lifetime of the plant below 20 μm/a. By contrast, the outlets indicated rates up to 150 μm/a.

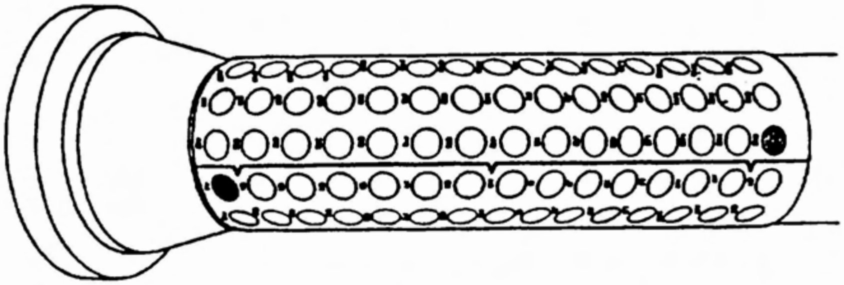

Figure 1. Flexible Template for Ultrasonic Gauging of Feeders.

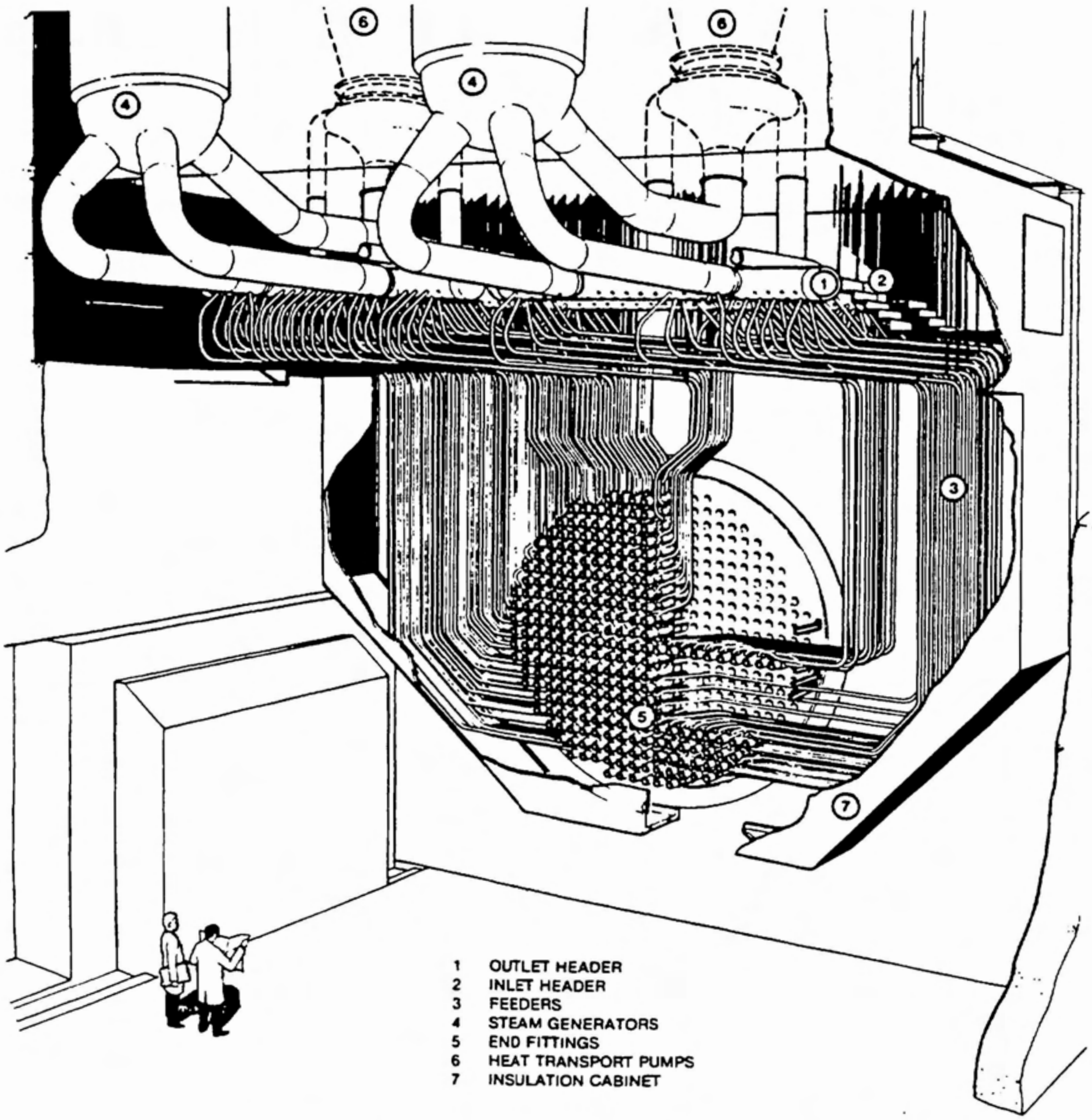

Figure 2. Arrangement of Feeders and Headers.

2. Steam quality does not seem to affect thinning rate. Over the range of average steam qualities below 4% that have been calculated with the NUCIRC code(4), no consistent effect on thinning rate has been detected.

3. The circumferential variation in thinning rate at the bends is between about 15% and 80%, with the maximum generally close to the bend extrados.

4. The axial variation in thinning rate over the first 3 m or so is less than about 20%, as indicated by the measurements on feeder F11. This observation, along with the previous two, is somewhat surprising given that the thinning phenomenon is expected to be sensitive to fluid turbulence effects, which should be much more severe at the bend extrados and be markedly affected by steam quality.

5. Thinning rates are correlated quite strongly with coolant velocity. For example, the values measured at the first bend extrados for both 2" and 2½" feeders together indicate a correlation with linear velocity raised to the power 1.52(5), though the data are quite scattered (see Figure 3). If only the 2" feeders at the corresponding location are considered a correlation with velocity raised to a power closer to unity can be obtained (6), though the scatter for these data is again high. It should be noted here that the coolant velocity used in the correlations is an average calculated with NUCIRC(4) over a channel fuelling cycle, taking into account the effects of steam quality variations with fuel burnup.

6. At positions away from the reactor face (i.e., close to the outlet header where the routine survey measurements have been made) thinning rates are low. This explains why the excessive thinning was not detected earlier, but raises the question of why the thinning should decline only after about 3 m beyond the outlet Grayloc, which was the distance scanned on F11. Certainly, some of the feeders measured at the header are of larger diameter there than closer to the reactor, so they would contain coolant of lower velocity; however, several of the monitored 2" feeders are the same diameter throughout their length, though these particular feeders contain coolant at the lower end of the velocity range and would not exhibit the fastest thinning rates anyway.

7. The chromium content of the steel is important. The piping is made of carbon steel, designated ASTM A106-B, and this material has an upper limit on chromium content of 0.40%. The specification for the PLGS feeders, however, was made with a view to minimizing activity transport, so low-cobalt material was procured. This necessarily minimized the chromium content, too, leading to concentrations of 0.02 - 0.03% Cr; analysis of the removed section of pipe indicated that S08 had a chromium content of 0.02%. The Grayloc hub on S08, however, contained 0.13% Cr, and the weld joining the hub to the pipe contained an intermediate concentration of 0.07%. Detailed examination of sections through the hub-feeder weld of S08 showed that the thinning was minor for the Grayloc, and increased stepwise to the pipe. This is a strong indication that chromium content is an important parameter in the thinning phenomenon, and that the specification of chromium content at the upper end of the permitted range for A106-B for future CANDU feeders should alleviate the thinning problem.

8. The accelerated thinning leads to a "scalloped" or "dimpled" surface with only a thin oxide

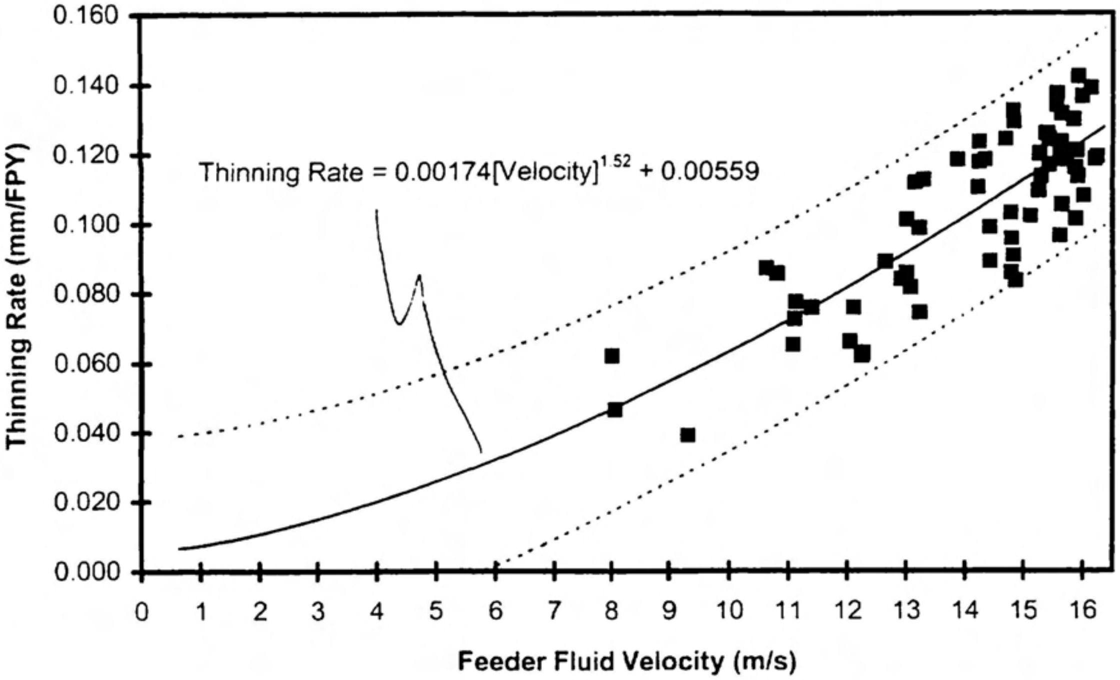

Figure 3. Thinning Rate at Extrados of First Bend on 2″ and 2.5″ Feeders at Point Lepreau.

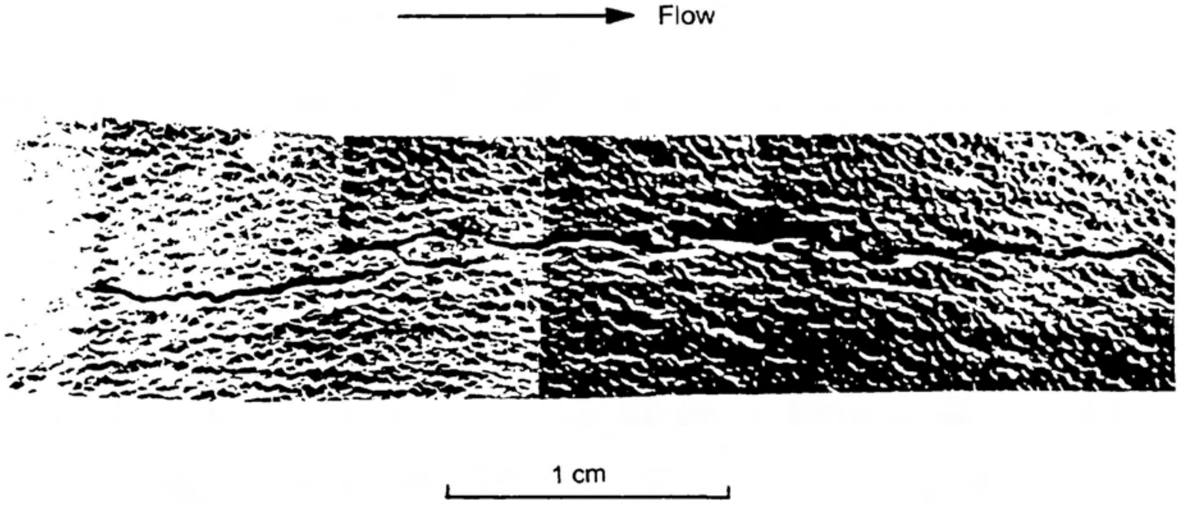

Figure 4. Surface of First Bend Intrados of Feeder S08 at Point Lepreau.

layer. Figure 4, taken from a microscopic investigation of the S08 feeder at the intrados of the first bend where the crack occurred, indicates that the scallops are roughly 0.5 - 0.75 mm across and appear to be in an overlapping pattern that follows the principal direction of the fluid flow. Metallographic sections reveal scallop depths of about 0.2 mm and an oxide film about 1 μm thick. Such surface scalloping is typical of the attack by flow-assisted corrosion (FAC) of carbon steel in feedwater systems(7) or even of the sculpting of clay, mud or rock river beds by fast-flowing streams(8).

THEORY - THE FAC APPROACH

The accelerated thinning of CANDU outlet feeders has many features in common with the rapid attack of carbon steel piping in feedwater systems, which is attributed to FAC - sometimes called erosion-corrosion (E-C). The fundamental premise is that the oxide film that forms on the carbon steel in high-temperature water protects the metal and limits the corrosion. Under normal circumstances, in carbon steel systems that contain coolant water saturated in dissolved iron, oxide films are thick. They are composed mostly of magnetite, Fe_3O_4, especially if the coolant chemistry is reducing. Corrosion of the underlying steel produces more oxide; at the metal-oxide interface Fe_3O_4 precipitates directly to occupy the volume of the metal corroded, while the remaining Fe^{2+} ions (constituting about 50% of the total corroded iron) emerge through pores at the oxide-coolant interface and precipitate there. This forms a double-layer oxide, with Fe_3O_4 crystals in the outer layer being somewhat larger than the fine grains in the inner layer(9).

There is evidence that such oxide films formed in iron-saturated water are modified by high coolant velocities. Thus, tests by AECL in a loop at the Sheridan Park Laboratory indicated that carbon steel piping subjected to CANDU coolant simulated with light water at 300°C developed double-layer oxides in coolant flowing at 12 m/s and 23 m/s, with the oxide in the latter being somewhat thinner than that in the former. In coolant at 36 m/s, however, only a single layer of very thin oxide was produced(3).

The explanation for these observations was that the erosive effect of the high coolant velocity continually spalled the oxide, with the higher velocity clearly having the greater effect. It is interesting to note that no consistent differences in corrosion rate could be discerned among the piping sections subjected to the different velocities; apparently, this was because the weight-loss technique that was employed on the large piping sections was too inaccurate to provide very meaningful results, and led to a large scatter in the data (up to two orders of magnitude).

The usual description of FAC processes postulates that if the coolant is not saturated in dissolved iron, dissolution will cause the oxide film to be thin. Thus, if mass transfer to the bulk coolant of the iron ions emerging from the oxide pores at the metal-oxide interface is faster than oxide precipitation, no outer layer will form; furthermore, the oxide film itself may be continuously dissolving at a rate that depends on the concentration driving force in the fluid boundary layer. We can visualize the establishing of a steady-state thickness, in fact, when the oxide formation at the metal-oxide interface equals its dissolution at the oxide-coolant interface. The link with coolant flow in this description is clear; increasing the fluid velocity increases the mass transfer coefficient and this increases the flux of dissolved iron to the bulk coolant. Places where very high turbulence occurs, such as orifices, sharp bends or elbows, etc., are expected to be particularly vulnerable because of the resulting high mass transfer coefficients.

In secondary coolant systems and feedwater lines in steam plants in general, the conditions of undersaturation in dissolved iron and high velocities are found frequently, particularly in the condensing steam sections. Problems with FAC in such systems have been widespread, and have led to catastrophic accidents in a few instances (in 1986, for example, a suction line to a feedwater pump at the Surry-2 PWR failed(10), causing several fatalities).

Studies of the FAC phenomenon in feedwater systems have spawned several mathematical models of the mechanism described briefly above (see the publications from the French (11) and British (12) industries for examples). The obvious similarities with the feeder thinning phenomenon have led to feeder models based on the same principles. Thus, the outlet feeders contain high-velocity water (between 8 m/s and 16.5 m/s) and there are regions of very high turbulence at the Grayloc connection to the fuel channel and the first two bends immediately downstream. The coolant is also undersaturated in dissolved iron because it is heated from 265°C to 310°C in the core, where there is no source of iron from the Zircaloy components. Over this temperature range, the solubility of magnetite in CANDU coolant increases from about 4 μg/kg to about 7.4 μg/kg(13) in terms of dissolved Fe, so the coolant leaves the core undersaturated in iron to the extent of about 3.4 μg/kg. (It should be noted here that other work has produced different solubility values for magnetite under these conditions(14); an increase with temperature is still predicted, however, even though the absolute values may be an order of magnitude different.) The effects of chromium in feeders are also expected to be like those in feedwater systems, where Cr-containing materials are often specified to counteract FAC. The effects depend upon the highly insoluble nature of Cr-based oxide. As oxide is continuously formed and dissolved on a steel containing Cr, the Cr left behind in the oxide concentrates and makes the film more protective. This is presumably what happened on the Grayloc hub and (to a lesser extent) the weld on feeder S08 at PLGS.

The modelling usually considers a steady-state thickness of the oxide film. If half of the corroded iron precipitates at the metal-oxide interface and half diffuses through the film, and if the dissolution of the oxide depends upon the undersaturation in dissolved iron in the coolant at the oxide surface, the corrosion rate can be derived simply in terms of the undersaturation in iron of the bulk coolant as:

$$\dot{m} = \frac{k_m . k_d}{(0.5k_m + k_d)} (C_{sat} - C_b) \qquad (1)$$

where

$\dot{m}$ = corrosion rate;
k_m = mass transfer coefficient;
k_d = magnetite dissolution kinetic constant;
C_{sat} = iron saturation concentration;
C_b = iron concentration in bulk coolant.

In this description of two processes in series - dissolution and mass transfer - the controlling process will be the one with the smaller kinetic constant. For example, if $k_d << 0.5\ k_m$, Equation (1) simplifies to:

$$\dot{m} = 2k_d\ (C_{sat} - C_b) \qquad (2)$$

the corrosion rate has no dependence on mass transfer and flow will have no effect. Using a published value (15) of magnetite dissolution rate constant in a slightly more detailed version of Equation (1), Lister et al(16) found that in fact dissolution was predicted to control carbon steel corrosion in CANDU coolant. They attempted to introduce a flow dependence by invoking a spalling mechanism based on the findings of the AECL tests(3). The predictions have fallen far short of the feeder thinning observations, however, even though the overall circuit balance for transported iron corresponded quite well with measurements of iron deposits inside steam generator tubes.

Equation (1) can also form the basis for a comprehensive model of corrosion and iron transport around a CANDU circuit if mass transfer controls(17). In this case, Equation (1) simplifies to:

$$\dot{m} = k_m\ (C_{sat} - C_b) \qquad (3)$$

and the corrosion rate depends upon coolant flow via mass transfer correlations such as (18):

$$Sh = 0.0165\ Re^{0.86}\ Sc^{0.33} \qquad (4)$$

where Sh = Sherwood Number

= $k_m\ d/D$ (d is pipe diameter and D is liquid phase diffusivity);

Re = Reynolds Number

= du / ν (u is fluid velocity and ν is kinematic viscosity);

Sc = Schmidt Number

= ν / D

THEORY - THE MODIFIED FAC APPROACH

A limitation of the straightforward FAC description is that the velocity dependence can be no greater than that dictated by the mass transfer correlation. For example, if Equations (3) and (4) were applicable, the thinning rate would depend upon $u^{0.86}$. If, however, Equation (4) applied but the mechanism were under mixed control, with $0.5\ k_m$ of comparable magnitude to k_d in Equation (1), then k_m would have less of an influence and the thinning rate would depend upon coolant velocity raised to a power between 0 and 0.86.

To avoid this limitation and to produce a mechanism that can explain a high velocity dependence such as that of the PLGS thinning data in Figure 3, we have assumed that oxide dissolution and mechanical erosion act in concert. In other words, we postulate a synergy between dissolution and erosion.

Thus, in coolant undersaturated in dissolved iron the oxide film on the surface of a carbon steel feeder pipe develops, as described earlier, by magnetite precipitation at the metal-oxide interface. This forms the protective oxide film, the thickness of which governs corrosion by impeding diffusion. Assuming that the oxide has theoretical magnetite density and just fills the volume of metal corroded, the actual amount of corroded iron that precipitates is 43%(16). The remaining 57% diffuses through the oxide and is transported to the bulk coolant (by convective processes described by the mass transfer coefficient) as it emerges from the pores at the oxide-coolant interface. At the same time, the oxide is dissolving and the resulting iron ions are also transported to the bulk coolant at a rate determined by the mass transfer coefficient. The concentration of dissolved iron in the bulk coolant therefore increases along the pipe in the downstream direction, so the concentration driving force for dissolution and transport diminishes with distance (note, however, that from a simple oxide dissolution/precipitation model Burrill and Turner(19) have concluded that the reactor outlet coolant in CANDU feeders remains undersaturated in dissolved iron - under normal chemistry conditions - all the way to the steam generators and for some distance into the steam generator tubes; measurements of steam generator deposits bear this out).

As corrosion proceeds and the oxide dissolution process continues, the film gets progressively weaker, even as it thickens by precipitation at the metal-oxide interface. Eventually, the fluid shear forces overcome the cohesive forces in the oxide and spalling occurs. Such spalling makes the film thinner and less protective, so the corrosion rate is increased. Again, however, the film thickens and is made weaker by dissolution until, as before, the critical thickness is reached when spalling occurs and the whole process is repeated.

In reality, the spalling will occur randomly over the surface in small patches. In time, some regular pattern of attack, dependent upon local flow and turbulence, may emerge and give rise to the scalloped surface as seen on feeder S08 at PLGS (as mentioned earlier, dissolution and erosion processes are known to create scalloped surfaces that depend on flow conditions(8); the scalloped pattern at PLGS is consistent with the scale of turbulence in the feeder flow). For the sake of the modelling, however, the equivalent situation is assumed; viz., the whole surface oxidizes and spalls as one unit. While this will not occur in practice the average effect is the same as that of the random process, and the mathematics are easier.

For the corrosion, film build-up and dissolution we follow the equation derivations of Reference (16). In summary, they amount to the following (continuing the nomenclature of the previous equations): the rate of diffusion of corroded iron through the oxide film is written . . .

$$0.476\,\dot{m}\,(1.101 + \phi) = \frac{D(C_{sat} - C_s)\rho\phi(1 - \phi)}{\delta \cdot \tau} \qquad (5)$$

where ϕ = oxide porosity;

ρ = oxide density;

τ = pore tortuosity factor;

C_s = concentration of dissolved Fe at oxide-coolant interface;

δ = oxide film "thickness" (mass / unit area).

The balance of dissolved iron at the oxide surface is . . . .

$$0.476\,\dot{m}\,(1.101 + \phi) + k_d F\,(C_{sat} - C_s) = k_m(C_s - C_b) \qquad (6)$$

where F = surface roughness factor $(\equiv \sqrt{3}$ for regular octahedra$)$ and the balance of iron in the oxide film furnishes the relation between corrosion rate $\dot{m}$ and film growth rate $\dot{\delta}$ as ...

$$0.723\,\dot{\delta} = 0.476\,\dot{m}\,(1 - \phi) - k_d F\,(C_{sat} - C_s) \qquad (7)$$

Equations (5), (6) and (7) allow the corrosion rate and film thickness to be calculated in terms of the bulk coolant iron concentration, C_b, as long as variations in C_b along the length of a feeder have a negligible effect on the surface processes. The actual variation in C_b with time t and length x comes from the equation . . .

$$\frac{\partial C_b}{\partial t} + u \cdot \frac{\partial C_b}{\partial x} - \frac{4k_m}{d}(C_s - C_b) = 0 \qquad (8)$$

where d is the pipe diameter.

We obtained most of the values of the constants in the equations from the literature as described in Reference (16). For oxide porosity, ϕ, we assumed 0.1 and for tortuosity, τ, 2. It should be noted here that the saturation concentration of iron, C_{sat}, was obtained from Sweeton and Baes$^{(13)}$; however, for C_{sat} in Equation (5), which is the equilibrium concentration at the bottom of a pore, the value is likely to be different from the corresponding value in the bulk coolant. To account for this, the treatment of Reference (16) involving the generation of dissolved hydrogen by corrosion was employed.

The computer solution of the equations generates corrosion rates and film thicknesses as functions of time. Because the magnetite dissolution constant from Reference (15) is considerably smaller than the mass transfer coefficient from References (16) and (18), dissolution controls and there is little effect of coolant flow. Correspondingly, this mechanism based solely on soluble iron transport would predict that corrosion rates are low.

We introduce erosion by postulating that the oxide film thickens according to the equations presented above until a critical thickness, δ_c, is reached, at which point spalling occurs to a minimum, δ_m. We assume that δ_c is inversely proportional to fluid shear stress at the wall, σ, where σ is related to the Reynolds Number by a relationship for friction factor, f....

$$f = \frac{\sigma}{\rho u^2} = \text{fun (Re)} \qquad (9)$$

Therefore,

$$\delta_c = \frac{A}{\rho u^2 \, \text{fun (Re)}} \qquad (10)$$

where A is a proportionality constant.

The Reynolds Number function, fun (Re), is obtainable from the text-book Stanton-Pannell or Moody diagrams; for Re $\geq 5 \times 10^6$ and high relative roughnesses of the pipe surface, it can be assumed to be a constant.

For a feeder with coolant of velocity 16.5 m/s, we achieved a good fit to the reactor data by choosing values of δ_c and δ_m of 2.1 μm and 0.9 μm respectively (i.e., indicating an "average" of 1.5 μm). Introducing these into the computer solution of Equations (5) - (8) produces a description of the oxide film that spalls every 80 h on average and sustains a corrosion rate of 130 μm/a. Since the constant in Equation (10) can now be fixed, we can compute the δ_c values for other feeders and velocities if δ_m is assumed constant. For example, for a feeder with 8.0 m/s coolant, we predict the film to grow to 10.1 μm before it spalls to 0.9 μm; this occurs every 2200 h on average, sustaining an average corrosion rate of 40 μm/a.

Figure 5 illustrates the oxide film behaviour under these two flow conditions. Again, we stress the point that this illustration is only the net effect of what in reality will be a series of random events occurring in discrete patches over the whole feeder surface. Note that if other solubility data and dissolution kinetics were chosen for input to the equations so that mass transfer had some influence, the curves of oxide growth between spalling events would be different for the different velocities.

We have also computed corrosion rates for the range of coolant velocities of the outlet feeders. In Figure 6, the predictions are superimposed on the measurements from PLGS. The fit is reasonable.

It is interesting to consider the input to the coolant of the predicted corrosion and film growth processes shown in Figures 5 and 6. For example, from the 16.5 m/s computation we calculate that over a 15 m length of outlet feeder pipe 2.0 μg/kg of dissolved Fe is added to the coolant concentration (99% of which is the corroded iron that diffuses through the oxide and 1% of which is from oxide dissolution) while 1.8 μg/kg of particulate crud are contributed (from spalling). At 8 m/s, however, 0.35 μg/kg of dissolved Fe (97% diffusing through the film and 3% dissolving off the film) and 1.0 μg/kg of crud are produced. We expect the dissolved Fe and the crud to behave differently in reactor coolant, so they should be treated differently in attempts to balance iron inventories around the coolant circuit.

EXPERIMENTAL

We have performed a preliminary scoping experiment in a high-temperature water loop that is involved in a series of PWR studies. The loop is a once-through pressurized system running with a positive-displacement pump of 7 L/min capacity; the feedtrain portion is made of stainless steel tubing and heated autoclaves. Coolant is conditioned at room temperature for pH and dissolved hydrogen in a 220 L feed tank before being fed to the pump. The flow leaves the stainless steel feedtrain at 265°C and enters the "inert" test section which comprises three 1 L-capacity titanium autoclaves which can be valved-in in series or in parallel using all-titanium or Zircaloy tubing and fittings. The first of these test-section autoclaves in the experiment served to heat the coolant to ~310°C before it entered the other titanium autoclaves where the PWR experiment was mounted.

At the downstream end of the test section, at the exit of the third titanium autoclave, we installed a titanium fitting that was designed to hold a carbon steel plug machined from a section of

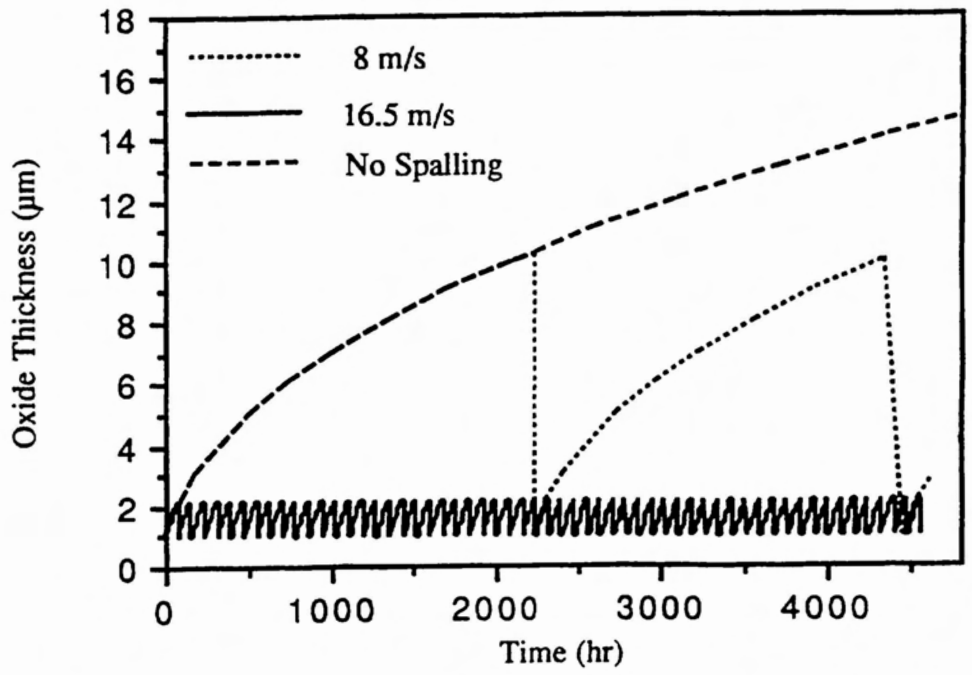

Figure 5. Computed Curves Showing the Net Effect of Spalling on Oxide Growth on Outlet Feeders.

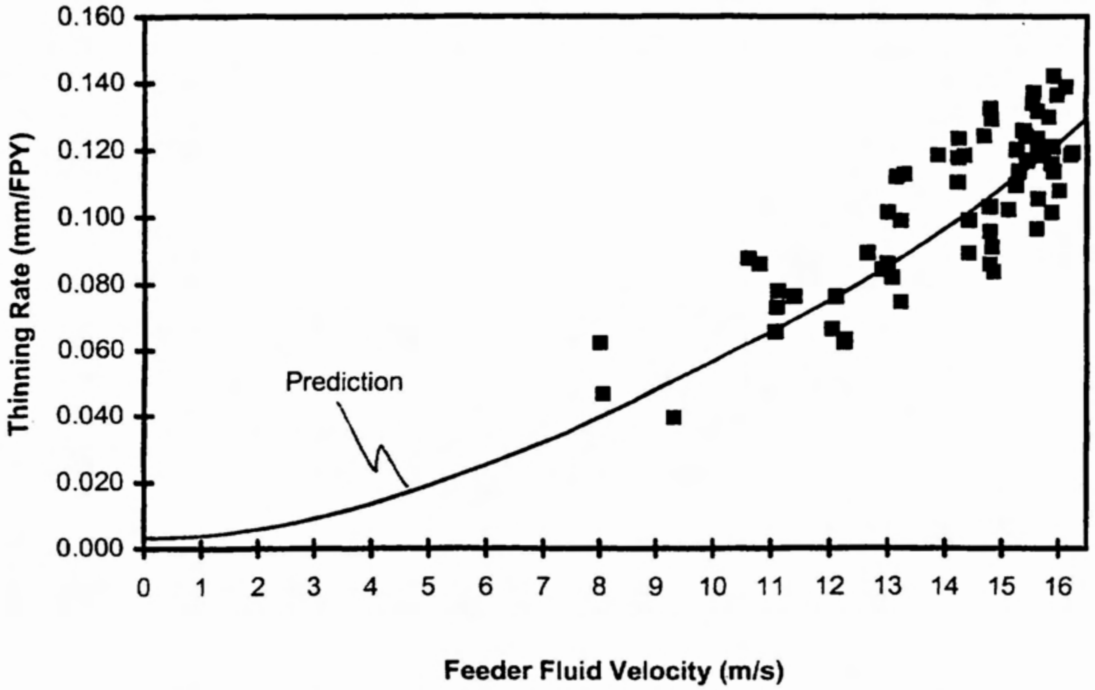

Figure 6. Curves of Predicted Corrosion Rates Superimposed on Thinning Data from Point Lepreau.

A106-B piping. The coolant entering the fitting was forced through a type 316 stainless steel orifice of 0.76 mm diameter to create a jet that was directed onto the surface of the plug about 1 cm away at a 45° angle (see Figure 7). The exiting coolant was directed back to the feed tank via heat exchangers, coolers and a pressure control valve. Just before entering the tank the returning coolant was passed through an ion exchange column containing lithiated, mixed-bed resin.

For the experiment reported here, the following conditions of the coolant at the carbon steel plug were maintained:

temperature	308±1 °C
jet velocity	18.5 m/s
pH_{RT} (LiOH)	10.6
dissolved hydrogen	18 cm^3/kg
dissolved oxygen	< 4 µg/kg

These conditions were designed to impose on the carbon steel surface a high velocity of coolant undersaturated in dissolved iron to the extent of 4 - 5 µg/kg(13). This is expected to be higher than the undersaturation in a CANDU coolant, where the pH nowadays is usually maintained towards the low end of the range 10.2 - 10.8, where the solubility of magnetite is lower. Before installation in the titanium fitting the surface of the plug was polished to a 600 grit SiC finish, its thickness measured by staff of RPC with an ultrasonic gauge and its surface profile scanned with a Talysurf. After installation of the plug the loop was started up and brought to steady conditions with the test section by-passed. When smooth operation was attained the whole inert section, including the titanium fitting with its carbon steel plug, was valved in. For a few days after the start of the experiment the plug was monitored with an on-line ultrasonic thickness gauge; the coolant was sampled periodically throughout the experiment and tested for dissolved oxygen with the Chemets colorimetric method and for pH.

The run lasted 930 h, after which the test section was valved out quickly and the loop run on the by-pass while the heating was switched off and the system cooled down. After the plug was removed it was examined with both an optical microscope and a SEM. It was then descaled by exposure for 1 minute in an inhibited solution of hydrochloric acid before being measured with the ultrasonic gauge and scanned with the Talysurf.

After removal from the loop the carbon steel surface was dark grey to black and had some minor striations perceptible downstream of the jet impingement point in the centre. Examination in the SEM revealed a dense, fairly uniform coating of equiaxed crystals, each 2 - 4 µm across (see Figure 8). In some areas, clumps of crystals appeared to have spalled off to uncover a fairly uniform substrate. There were a few pits on the surface that had been created before exposure during the initial ultrasonic gauging, and these too were coated with the crystals. Microscopic examination of the orifice plate indicated that no crystals had deposited there and that there had been no observable attack of the orifice itself.

Elemental analysis of the crystals by EDX indicated similar concentrations of iron and titanium

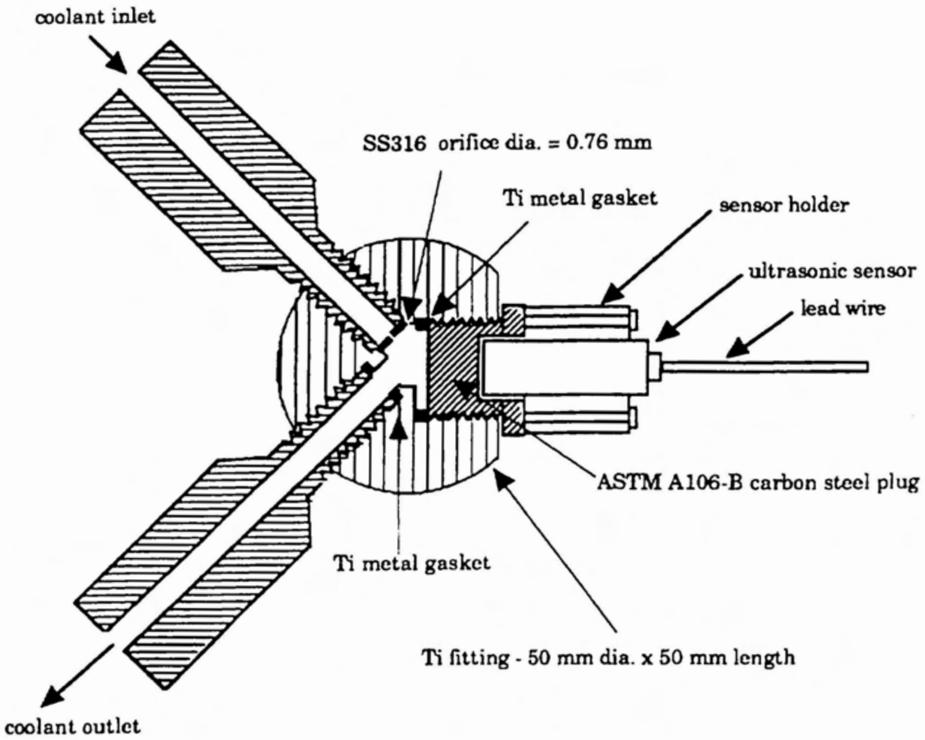

Figure 7. Carbon Steel Plug in Titanium Insert in High Temperature Loop.

Figure 8. SEM Picture of Jet Impact Area on Carbon Steel Plug.

(Ti / Fe = 0.87 - 0.89); since the overall thickness of this layer of crystals was about 5 μm or more, the EDX analysis should have no interference from the underlying metal.

The presence of the layer of oxide crystals indicates that a 18.5 m/s jet of coolant undersaturated in dissolved iron could not suppress the precipitation of an outer-oxide layer. That this oxide was titanium-rich indicates that the coolant must have picked up titanium ions from the surfaces of the fittings and components in the loop upstream of the carbon steel plug. Presumably, at the surface of the carbon steel, the input of iron from corrosion and the input of titanium in the coolant created supersaturated conditions for the precipitation of an oxide - probably ilmenite, $Fe\,Ti\,O_3$, though there is also the possibility of precipitating an inverse spinel(20) $Fe\,(Ti\,Fe)\,O_4$.

The Talysurf scans indicated that the exposure had slightly roughened the surface in the area of the jet impaction, but no appreciable loss of metal was evident. The ultrasonic gauging before and after exposure was inconclusive from the standpoint of measuring metal loss because of changes in measurement geometry; however, the on-line ultrasonic gauging at the beginning of the exposure demonstrated the durability of the sensor at high temperature.

DISCUSSION

The semi-empirical model we describe above seems to have the major features needed for successfully describing the reactor phenomena. It contains the elements of FAC, which involve oxide dissolution and mass transport, interacting synergistically with mechanical erosion. The former introduces dissolved iron to the coolant while the latter introduces crud. The few μg/kg levels predicted seem to be in the range of reactor observations, but this is not surprising in view of the correspondence of the predicted corrosion rates with reactor observations. However, the separation in the model of the crud and dissolved species, which should have different transport behaviour, offers the possibility of at least partially accounting for difficulties in reconciling known feeder corrosion rates with iron deposits in the steam generators.

The model is also consistent with overall velocity trends at PLGS; detailed turbulence effects, including the influence of steam bubbles, can be included in terms of local fluid shear stress and mass transfer coefficient. Preliminary indications are that such local effects, in terms of the scale of turbulence at the feeder pipe surface, are consistent with the scalloping found on S08 at PLGS.

While the model seems promising, some refinement is probably in order. For example, the concept for all feeders of a fixed minimum thickness of oxide after spalling, δ_m in the equations, might be improved if more information from operating feeders at different coolant velocities were available or if more experiments had been performed. Also, it would be useful to test the model with different values of oxide solubility and dissolution rate constant to investigate further the interplay of erosion and mass transport.

Clearly, the model supports the possibility of counteracting feeder thinning by controlling oxide dissolution. We again emphasize the point that dissolution is key to the mechanism by weakening the oxide film so that it spalls. If pH were adjusted downward to an oxide precipitation range, then like the conventional FAC descriptions the model would predict no accelerated corrosion. Similarly, chromium in the steel would act to reduce predicted thinning rates by interfering with the oxide dissolution term in the model.

The observation of the titanium-rich crystals on the carbon steel surface in the experiment is intriguing; the crystals have clearly survived the severe turbulence caused by the impact of a 18.5 m/s jet undersaturated in dissolved iron, and they seem to have imparted some protection to the metal (the Talysurf profile showed little attack, and a rough calculation of the amount of corrosion required to form the 5 μm - thick layer indicates a corrosion rate of about 11 μm/a). This raises the possibility of introducing titanium into an operating reactor circuit to protect the carbon steel.

From an activation point of view, titanium should be benign in a reactor system, and there should be no problems with galvanic effects on system components. The dificulty appears in visualizing a system for introducing titanium ions into solution, for the solubility of titanium species in water is very low. In fact, our initial theoretical estimates, which are based on the methodology of Macdonald et al(21), indicate a solubility for titanium several orders of magnitude below that of iron at the same temperature. Because of large uncertainties in the scarce thermodynamic data available for the solubility calculations, the final estimates no doubt contain a large error. Nevertheless, we have never seen titanium in loop coolant samples analysed with inductively-coupled-plasma spectrometry, so remain convinced of the low solubility. In any case, it is clear that titanium transport did occur in the loop, and it is likely that interaction with iron ions at the corroding steel surface deposited the mixed-oxide layer. We suggest that this could be a fruitful area for further study.

MAJOR CONCLUSIONS AND RECOMMENDATIONS

1. The thinning data from the outlet feeders at Point Lepreau indicate:
- a strong correlation with coolant velocity;
- little effect of two-phase flow;
- an ameliorating effect of chromium content of the carbon steel.

2. The reactor observations can be described by a semi-empirical model that invokes oxide dissolution, driven by undersaturation in dissolved iron in the coolant, and oxide spalling. These processes work together and act as sources of dissolved iron and crud. Refinements to the model require detailed information on corrosion and oxide growth under coolant conditions of high velocity and undersaturation in dissolved iron.

3. The model, like the conventional flow-assisted corrosion mechanism, suggests that any measure to reduce magnetite dissolution, such as reducing coolant pH, would ameliorate the thinning.

4. A high-temperature loop experiment has indicated that coolant-borne titanium can co-precipitate with iron as an oxide film on the surface of carbon steel, even when the steel is

subjected to high coolant velocity and turbulence (via a liquid jet) and the coolant is undersaturated in dissolved iron. The mixed-oxide film apparently protected the carbon steel from accelerated corrosion in the experiment. This suggests that titanium might be effective as an additive to alleviate the thinning problem in operating reactors. Considerable research is needed first.

ACKNOWLEDGEMENTS

We are grateful to NB Power for permission to use the Point Lepreau information, and to the Nuclear Installations Inspectorate (U.K.) for allowing the carbon steel experiment to be added to the PWR series. We would also like to thank J. McInerney of the University of New Brunswick for designing the titanium insert and operating the loop, and M. Beshara of N.B. Power for collating much of the data.

REFERENCES

(1) BERRY, W.E., "Corrosion in Nuclear Applications", John Wiley and Sons, Inc., 1971.

(2) VIDEM, K. and Aas, S., "Mild Steel in Primary Circuits in Water Cooled Power Reactors", Kjeller Report KR-39, 1963.

(3) PEARSON, B.M., MURPHY, E.V., JACKSON, G.W. and HENDRIE, G.F., "Single-Phase Liquid Erosion/Corrosion Test Program", AECL Report IR-522, 1984 March.

(4) HARVEL, G., "Private Communication", AECL, 1996.

(5) BESHARA, M, "Accelerated Wall Thinning of CANDU Outlet Feeders", Proc. 22nd Annual CNA/CNS Student Conference, Fredericton, 1997 March 14-15.

(6) CHELUGET, E., "Private Communication", AECL, 1997.

(7) CHEXAL, B., HOROWITZ, J., JONES, R., DOOLEY, B., WOOD, C., BOUCHACOURT, M., REMY, F., NORDMANN, F. and ST. PAUL, P., "Flow Accelerated Corrosion in Power Plants", EPRI Report TR-106611, 1996.

(8) ALLEN, J.R.L., "Transverse Erosional Marks of Mud and Rock", Sediment. Geol., 5 , (3/4), 167, 1971.

(9) POTTER, E.C. and MANN, G.M.W., "Oxidation of Mild Steel in High-Temperature Aqueous Systems", Proc. 1st Interml. Congress Metall. Corrosion, London, 1962, p. 417.

(10) CZAJKOWSKI, C., "Metallurgical evaluation of an 18-Inch Feedwater Line Failure at the Surry Unit 2 Power Station", NUREG/CR - 4868, Brookhaven National Lab. 1987.

(11) BERGE, Ph., DUCREUX, J. and SAINT-PAUL, P., "Effects of Chemistry on Erosion Corrosion of Steels in Water and Wet Steam", Proc. 2nd BNES Internl. Conf. on Water Chem. of Nuclear Reactor Systems, Bournemouth, U.K. 1980.

(12) BIGNOLD, G.J., GARBETT, K., GARNSEY R. and WOOLSEY, I.S., "Erosion-Corrosion in Nuclear Steam Generators", Ibid.

(13) SWEETON, F.H. and BAES, C.F. Jr., "The Solubility of Magnetite and Hydrolysis of Ferrous Ion in Aqueous Solutions at Elevated Temperatures", J. Chem. Thermod., 2., 479, 1970.

(14) TREMAINE, P.R. and LEBLANC, J.C., "The Solubility of Magnetite and the Hydrolysis and Oxidation of Fe^{2+} in Water to 300°C.", J. Soln. Chem., 9, 415, 1980.

(15) BALAKRISHNAN, P.V., "A Radiochemical Technique for the Study of Dissolution of Corrosion Products in High-Temperature Water", Can. J. Chem. Eng., 55, 357, 1977.

(16) Lister, D. H., ARBEAU, N. and JOHARI, J.M.C., "Erosion and Cavitation in the CANDU Primary Heat Transport System", AECB Report, 1994, Issued as RSP-009, 1996.

(17) BURRILL, K.A., "Private Communication", AECL, 1996.

(18) BERGER, F.P., and HAU, K-F. F-L., "Mass Transfer in Turbulent Pipe Flow Measured by the Electrochemical Method", Internl. J. Heat Mass Trans., 20, 1185, 1977.

(19) BURRILL, K.A. and TURNER, C.W., "Control of Reactor Inlet Header Temperature (RIHT) Rise in CANDU", Proc. 2nd CNS/COG Internl. Steam Generator and Heat Exchanger Conf., Toronto, 1994.

(20) WELLS, A.F., "Structural Inorganic Chemistry", Third Edition, Clarendon Press, Oxford, p. 488, 1962.

(21) MACDONALD, D.D., SHIERMAN, G.R. and BUTLER, P., "The Thermodynamics of Metal-Water Systems at Elevated Temperatures. Part 2, Iron-Water Systems", AECL-4137, 1972.